3rd URSI AT-AP-RASC, Gran Canaria, 29 May – 3 June 2022

Variation of TEC Over South Africa During a Geomagnetic Storm

Tshimangadzo M. Matamba*(1) and Donald W. Danskin(2)
(1) South African National Space Agency (SANSA), P.O. Box 32, Hermanus, 7200, South Africa, https://www.sansa.org.za/
(2) Retired

Abstract

The ionosphere affects how radio waves propagate from the satellite to ground based receivers. During geomagnetic storms the Total Electron Content (TEC) varies due to the driving forces of the storm. The South African National Space Agency (SANSA) near-real time TEC map version 2 was used to show how the ionosphere varied during the geomagnetic storm of 19 - 23 Dec 2021. The Global Positioning System (GPS), ionosondes, and the quiet-time AFriTEC model were compared during the five day period. During the period of analysis, the Root Mean Squared Error (RMSE) were greater during the geomagnetic storm as compared with quiet days. The decrease in TEC were observed on 20 and 21 Dec 2021 during a geomagnetic storm period. The estimated TEC from the GPS and ionosode had similar temporal variations and magnitudes.

1 Introduction

The ionosphere effects the propagation of radio waves between satellites and ground based receivers. The GPS satellite network were designed to provide accurate time and position of near-Earth receivers. However, the variation of the ionosphere causes perturbations in the position estimates. Using dual frequency GPS, the Total Electron Content (TEC) can be estimated and provides a measure of the variability of the ionosphere [1]. The ionosphere is the region that extends from $\sim$50 km to $\sim$1000 km above the Earth surface and is formed by interaction between the extreme ultraviolet and X-rays solar radiation [2]. The variation of input radiation causes changes in the distribution of TEC with altitude, geographic coordinates and time. Another source of variation of TEC is the transport of the electron density by neutral winds and electric and magnetic fields.

The ionosphere can experience major disturbances during geomagnetic storms called ionospheric storms. The ionospheric storms are mainly caused by processes driven from sun's activities such as Corotating interaction regions (CIRs), HSSs, Solar Energetic-Particle (SEP), Coronal Mass Ejections (CMEs) and solar flares [2]. CIRs can drive perturbations in the solar wind density, speed and magnetic field. These solar wind perturbations may cause geomagnetic storms when they interact with Earth's magnetic field. The CIR-driven storms tends to occur mostly during the declining phase of the solar cycle, and also during the recurring 27-day high speed streams (HSSs) occurs throughout the solar cycle [3, 4, 5, 6].

South Africa through the South African National Space Agency (SANSA) has been recognized by the International Civil Aviation Organization (ICAO) to be a regional warning center to provide space weather information to the global aviation sector. To support ICAO space weather requirements, SANSA has developed a product that includes maps of TEC, spatial gradient, temporal gradient and ROTI. The version 2 TEC maps of SANSA are used in the investigation of a geomagnetic storm that gave a negative ionospheric storm over South Africa.

2 Methodology

For the near-real time TEC maps and other related products, the satellite biases were downloaded daily from the Center for Orbit Determination in Europe (CODE) website http://www.aiub.unibe.ch/download/CODE/. The method used by [7] was used to estimate receiver biases by minimizing the standard deviation of TEC during the quiet time of the day (02:00 - 05:00 LT). [8] noted that the day-to-day variability of receiver biases does not change significantly during quiet days but changes significantly during ionospheric active periods. Hence, the receiver bias is maintained at a fixed level for each receiver and only changes when the receiver is changed. The receiver biases remained fixed in order to see the ionospheric variability [8].

The Trignet (http://www.trignet.co.za/) RINEX files are downloaded and stored locally by the NTRIP caster each minute and were used to generate 15 minutes TEC maps that are updated every 5 minutes. The daily navigation file from Hermanus for the previous day were used for the satellites ephemeris.

The slant TEC values for 20 Trignet stations were verticalized based on elevation angle. The data was gridded to a 1° latitude $\times 1^\circ$ longitude and median filtered. The Root Mean Squared Error (RMSE) is computed between the verticalized TEC and the estimated TEC from the gridding process. Two quality factors are estimated to identify the amount of data in each map. The first quality factor is based on the

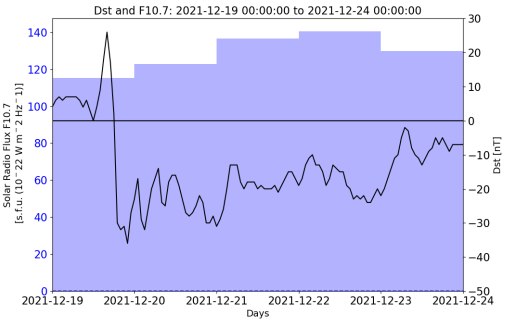

Figure 1. Dst (black, right axis) and F10.7 (blue, left axis) for 19 - 24 Dec 2021.

number of available stations out of the 20 desired stations. The second quality factor is the number of valid TEC values divided by the number of TEC values in the 15-minute period. As an added visual check on the validity of the maps, the measured TEC values are superimposed on the maps of TEC with the same color scale as the map. For each satellite and receiver pair, the measured TEC values appear as short linear segments as in Figure 2.

3 Negative storm event – 19 – 23 Dec 2021

Figure 1 illustrates the solar radio flux (F10.7) and disturbance storm time (Dst) indices for the storm period 19 - 24 Dec 2021. The sudden storm commencement happened on 19 Dec 2021 at $\sim$ 19:00 UT. The minimum Dst index reached $\sim$-36 nT at 22:00 UT. The Dst index remained at negative intensity for the next 3 days. The $F_{10.7}$ showed an increased level from 20 - 22 Dec 2021 and the maximum value was $\sim$140 s.f.u (10^{-22}Wm^{-2}Hz^{-1}).

Figure 2 shows the TEC maps during the daytime at 10:00 UT for 19 - 22 Dec 2021. Figure 2(a) shows how TEC is distributed on the typical day over South Africa. The stormy period began later in the day at $\sim$ 19:00 UT during the night time. (b) and (c) correspond to days during the geomagnetic storm mainly in the recovery phase. (d) is similar to (a) indicating that the geomagnetic storm has past. The map shows the gridded median filtered TEC with the TEC values at each IPP. The TEC at the IPPs use the same color scale as the TEC map. The black dots are the location of the stations used to produce the gridded TEC map with the station names labeled in white. In general, the TEC on the southern part of the South Africa is lower than the TEC on the northern part which is clearly visible on the maps. When there is a good agreement of the TEC at IPPs, the color blends well with the color of the TEC map. The TEC values ranged between $\sim$ 30 - 40 TECU, 20 - 26 TECU, 18 - 28 TECU and 28 - 36 TECU on the 19, 20, 21 and 22 Dec 2021 respectively. The TEC values displayed a depleted TEC values on 20 and 21 Dec 2021 whereas on 22 Dec 2021 the TEC values seem to recover from the storm.

The RMSE was computed based on the TEC from IPPs and the gridded estimated TEC using the traditional equation of RMSE. The RMSE values for the TEC maps were 2.65, 3.07, 3.16 and 2.46 as indicated on Figures 2(a), (b), (c) and (d) respectively for the period 19 - 22 Dec 2021. The RMSEs were less than 3 on 19 and 22 Dec 2021 during non-storm periods. The RMSE of the TEC maps were greater than 3 on 20 and 21 December 2021 during geomagnetic storm, which could indicate that the ionosphere is more variable during the ionospheric storm effect as observed on 20 and 21 Dec 2021.

The quality of the TEC maps with regards to the number of stations available indicates that $\geq$ 90% of the stations were used to compute TEC maps and more than 98% of TEC values that created the TEC maps were valid. The high values of quality indicate that the maps have sufficient data to be reliable.

4 Discussion

Figure 3 shows the estimated TEC values extracted from the near-real time TEC maps (HE13N_gps (black dots) and GR13L_gps (green dots)) were compared with ionosonde TEC (HE13N_iono (blue dots) and GR13L_iono (red dots)) and AfriTEC model [9, 10] (HE13N_AfriTEC (cyan) and GR13L_AfriTEC (magenta)). The top panel shows the daily variation of TEC values over a 5 day (19 - 23 Dec 2021) period over Hermanus (19.22°E, 34.42°S) and Grahamstown (26.50°E, −33.30°S).

The lower panels show the relationships of the TEC estimates with ionosonde TEC (black dots) and with AfriTEC (cyan dots) for Hermanus and Grahamstown stations left and right panels respectively. The cyan and black lines represents the best fit line for each pair whereas the black line represent the expected best fit line for each pair. The correlation coefficients (r) for the comparison of estimate TEC with ionosonde TEC are 0.90 and 0.95 for Hermanus and Grahamstown respectively. The slopes are 1.15 and 0.97 for Hermanus and Grahamstown respectively. With these slopes close to 1.0, the estimated TEC has similar variation as the Ionosonde TEC. Hence the ionosonde and the TEC maps give consistent results.

When comparing the estimated TEC with the AfriTEC model, the correlation coefficients for AfriTEC are 0.90 and 0.92 for Hermanus and Grahamstown respectively. However, the slopes are 0.64 and 0.66 for Hermanus and Grahamstown respectively. With these slopes being substantially less than 1.0 and remembering that AfriTEC is running a quiet time model during this event, clearly during the storm the TEC is depleted compared with the quiet time ionosphere. Hence, clearly the event is a negative ionospheric storm. The negative ionospheric storm effect over the mid-latitude region could be due to the changes in neutral composition [11, 12, 13]. Alternatively, transport of the electron density into the polar regions could also deplete the mid-latitude ionosphere [14].

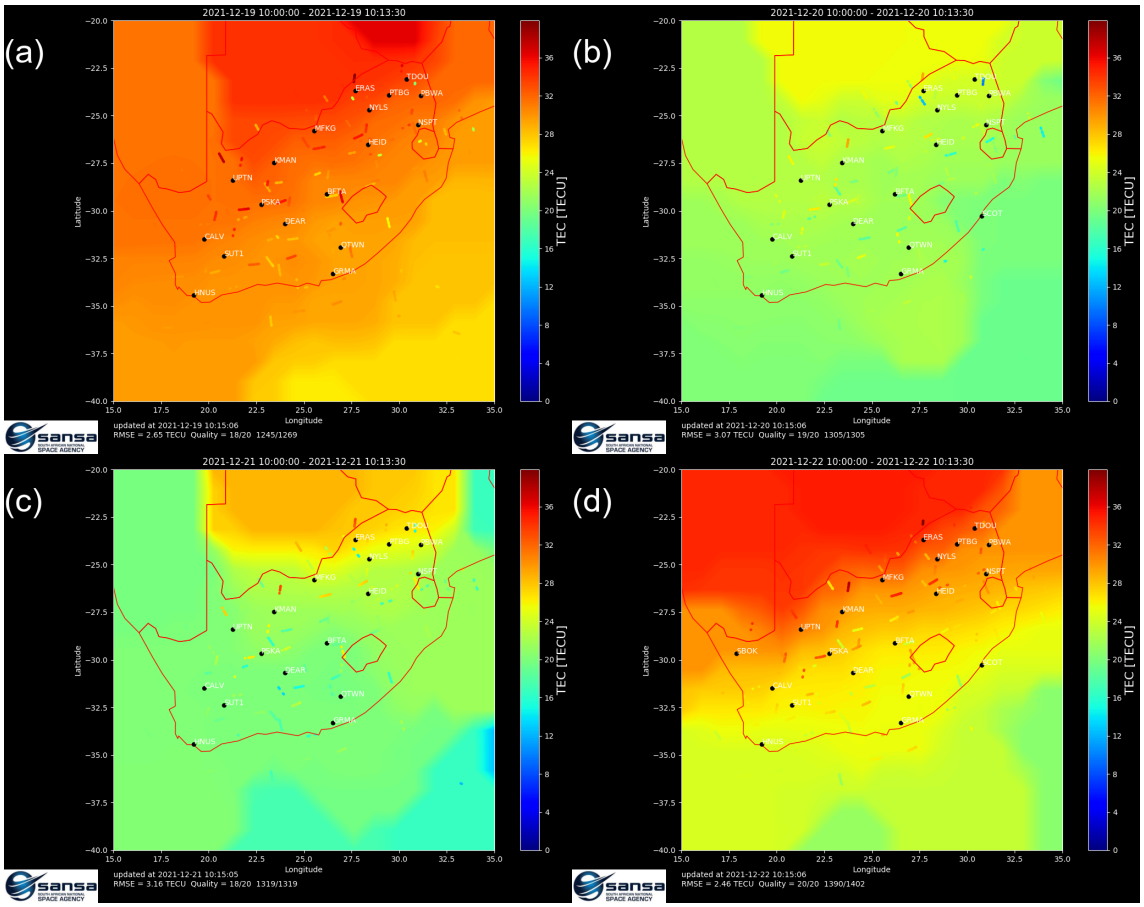

Figure 2. TEC maps on the following days at 10:00 UT: (a) 19 Dec 2021, (b) 20 Dec 2021, (c) 21 Dec 2021 and (d) 22 Dec 2021.

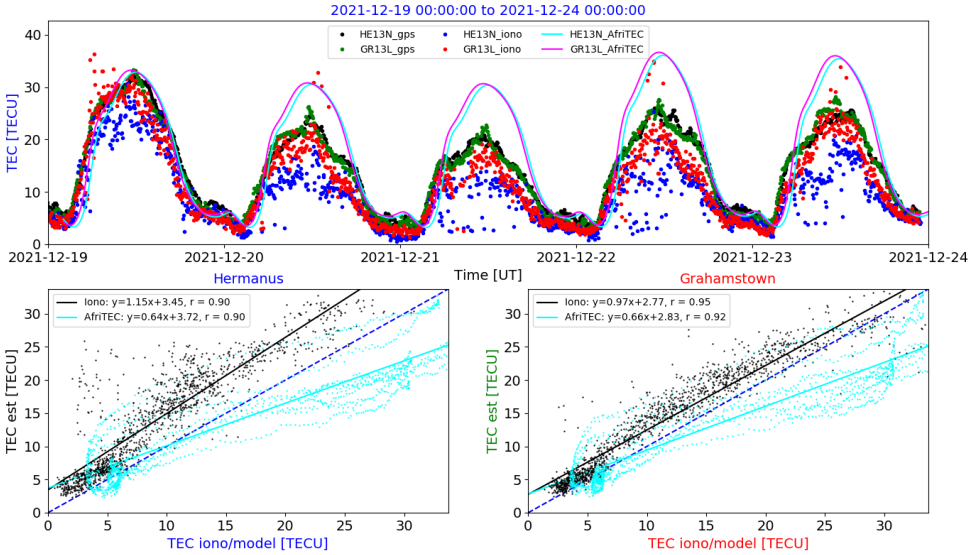

Figure 3. The TEC estimates from the ionosonde, AfriTEC and near-real time TEC maps for 19 - 24 Dec 2021. Lower left is the comparison of Ionosonde and AfriTEC with TEC estimated from the TEC maps over Hermanus. Lower right similar comparison for Grahamstown. The AfriTEC model is for quiet times.

5 Conclusion

An investigation using SANSA TEC maps version 2 during a geomagnetic storm has shown in this instance to generate a negative ionospheric storm. Before and after the storm, the maps of TEC appear similar with lower values of RMSE than during the storm. The negative storm effect is most pronounce during the daytime periods.

The comparison of TEC estimated from the GPS satellites always compared favorably with the estimates of TEC from the ionosondes. When compared with the AfriTEC quiet time model, the TEC was found to be substantially less than the model predicted. Hence the negative ionospheric storm occurred during the geomagnetic storm.

6 Acknowledgements

Authors would like to thank the South African National Space agency for their support. The GPS data used were provided by the Chief Directorate: National Geospatial information, South Africa (`http://trignet.co.za/`) via NTRIP. The satellite bias data were obtained from `http://www.aiub.unibe.ch/download/CODE/`. The ionosonde data can be obtained from `https://giro.uml.edu/didbase/`. The Dst index data used in this study were obtained from `http://wdc.kugi.kyoto-u.ac.jp/index.html` operated by Data Analysis Center for Geomagnetism and Space Magnetism. The F10.7 data was obtained from the GFZ German Research Centre for Geosciences, at `https://www.gfz-potsdam.de/en/kp-index/`. The authors would also like to acknowledge Jon Ward and Kate Niematinga for monitoring the near-real time data for TEC maps.

References

[1] R. Ghoddousi-Fard, P. Héroux, D. Danskin, and D. Boteler, "Developing a GPS TEC mapping service over Canada," *Space Weather*, vol. 9, no. 6, 2011.

[2] L. F. McNamara, *The ionosphere: communications, surveillance, and direction finding*. Krieger publishing company, 1991.

[3] A. Balogh, V. Bothmer, N. Crooker, R. Forsyth, G. Gloeckler, A. Hewish, M. Hilchenbach, R. Kallenbach, B. Klecker, J. Linker *et al.*, "The solar origin of corotating interaction regions and their formation in the inner heliosphere," *Space Science Reviews*, vol. 89, no. 1, pp. 141–178, 1999.

[4] J. E. Borovsky and M. H. Denton, "Differences between cme-driven storms and cir-driven storms," *Journal of Geophysical Research: Space Physics*, vol. 111, no. A7, 2006. [Online]. Available: https://agupubs.onlinelibrary.wiley.com/doi/abs/10.1029/2005JA011447

[5] B. T. Tsurutani, W. D. Gonzalez, A. L. Gonzalez, F. L. Guarnieri, N. Gopalswamy, M. Grande, Y. Kamide, Y. Kasahara, G. Lu, I. Mann *et al.*, "Corotating solar wind streams and recurrent geomagnetic activity: A review," *Journal of Geophysical Research: Space Physics*, vol. 111, no. A7, 2006.

[6] T. M. Matamba and J. B. Habarulema, "Ionospheric Responses to CME-and CIR-Driven Geomagnetic Storms Along 30° E–40° E Over the African Sector From 2001 to 2015," *Space Weather*, vol. 16, no. 5, pp. 538–556, 2018.

[7] G. Ma and T. Maruyama, "Derivation of TEC and estimation of instrumental biases from GEONET in Japan," in *Annales Geophysicae*, vol. 21, no. 10. Copernicus GmbH, 2003, pp. 2083–2093.

[8] T. M. Matamba, D. W. Danskin, and P. J. Cilliers, "Evaluation of Stability of GPS Satellite and Receiver Bias," in *2020 IEEE International Conference on Wireless for Space and Extreme Environments (WiSEE*. IEEE, 2020, pp. 78–82.

[9] D. Okoh, G. Seemala, B. Rabiu, J. B. Habarulema, S. Jin, K. Shiokawa, Y. Otsuka, M. Aggarwal, J. Uwamahoro, P. Mungufeni, S. Bolaji, O. Aderonke, E. Nada, O. Chinelo, T. Mpho, and S. Dadaso, "A neural network-based ionospheric model over Africa from Constellation Observing System for Meteorology, Ionosphere, and Climate and Ground Global Positioning System observations," *Journal of Geophysical Research: Space Physics*, vol. 124, no. 12, pp. 10 512–10 532, 2019.

[10] D. Okoh, J. B. Habarulema, B. Rabiu, G. Seemala, J. B. Wisdom, J. Olwendo, O. Obrou, and T. M. Matamba, "Storm-Time Modeling of the African Regional Ionospheric Total Electron Content Using Artificial Neural Networks," *Space Weather*, vol. 18, no. 9, p. e2020SW002525, 2020.

[11] G. W. Prölss, "On explaining the negative phase of ionospheric storms," *Planetary and Space Science*, vol. 24, no. 6, pp. 607–609, 1976.

[12] G. Prölss, "On explaining the local time variation of ionospheric storm effects," in *Annales Geophysicae*, vol. 11, no. 1, 1993, pp. 1–9.

[13] T. M. Matamba, J. B. Habarulema, and L.-A. McKinnell, "Statistical analysis of the ionospheric response during geomagnetic storm conditions over South Africa using ionosonde and GPS data," *Space Weather*, vol. 13, no. 9, pp. 536–547, 2015.

[14] G. W. Prölss, "Ionospheric F-region storms," in *Handbook of Atmospheric Electrodynamics, Volume II*. CRC press, 1995, pp. 195–248.